

Electrophysiological Phenotype in Angelman Syndrome Differs Between Genotypes

Joel Frohlich, Meghan T. Miller, Lynne M. Bird, Pilar Garces, Hannah Purtell, Marius C. Hoener, Benjamin D. Philpot, Michael S. Sidorov, Wen-Hann Tan, Maria-Clemencia Hernandez, Alexander Rotenberg, Shafali S. Jeste, Michelle Krishnan, Omar Khwaja, and Joerg F. Hipp

ABSTRACT

BACKGROUND: Angelman syndrome (AS) is a severe neurodevelopmental disorder caused by either disruptions of the gene *UBE3A* or deletion of chromosome 15 at 15q11-q13, which encompasses *UBE3A* and several other genes, including *GABRB3*, *GABRA5*, *GABRG3*, encoding gamma-aminobutyric acid type A receptor subunits ($\beta 3$, $\alpha 5$, $\gamma 3$). Individuals with deletions are generally more impaired than those with other genotypes, but the underlying pathophysiology remains largely unknown. Here, we used electroencephalography (EEG) to test the hypothesis that genes other than *UBE3A* located on 15q11-q13 cause differences in pathophysiology between AS genotypes. **METHODS:** We compared spectral power of clinical EEG recordings from children (1–18 years of age) with a deletion genotype ($n = 37$) or a nondeletion genotype ($n = 21$) and typically developing children without Angelman syndrome ($n = 48$).

RESULTS: We found elevated theta power (peak frequency: 5.3 Hz) and diminished beta power (peak frequency: 23 Hz) in the deletion genotype compared with the nondeletion genotype as well as excess broadband EEG power (1–32 Hz) peaking in the delta frequency range (peak frequency: 2.8 Hz), shared by both genotypes but stronger for the deletion genotype at younger ages.

CONCLUSIONS: Our results provide strong evidence for the contribution of non-*UBE3A* neuronal pathophysiology in deletion AS and suggest that hemizyosity of the *GABRB3-GABRA5-GABRG3* gene cluster causes abnormal theta and beta EEG oscillations that may underlie the more severe clinical phenotype. Our work improves the understanding of AS pathophysiology and has direct implications for the development of AS treatments and biomarkers.

Keywords: Angelman syndrome, Biomarkers, EEG, GABA, *GABRB3-GABRA5-GABRG3* gene cluster, *UBE3A*

<https://doi.org/10.1016/j.biopsych.2019.01.008>

Angelman syndrome (AS) is a rare genetic neurodevelopmental disorder with a prevalence of 1 in 10,000 to 24,000 births (1,2). Clinical traits of AS include global developmental delay, intellectual disability, microcephaly, epilepsy, sleep difficulties, and some phenotypic overlap with autism (3–6). The lack of functional ubiquitin-protein ligase E3A (*UBE3A*) in neurons underlies core features of AS as evidenced by the phenotype of individuals with point mutations solely affecting this gene (7–9). *UBE3A* is encoded by the eponymous gene *UBE3A* on chromosome 15 and is generally expressed only from the maternal allele in neurons but biallelically expressed in other cell types (8,10,11). The downstream consequences of *UBE3A* dysfunction are not understood in detail, but preclinical mouse models of AS show altered dendritic spine morphology (12,13) and impaired synaptic function (14–17) that may underlie global electrophysiological abnormalities of the electroencephalography (EEG) (15,18,19). These preclinical findings are in line with neuropathological case studies in individuals with AS that point to cellular abnormalities in cortical pyramidal neurons including irregular distribution, decreased dendritic arborization, a reduced number of dendritic spines (20,21),

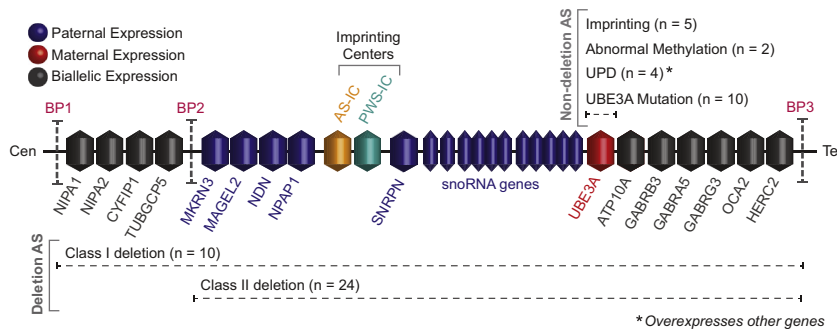
and a strongly abnormal EEG in AS (18,22–24). Despite these anomalies, the gross anatomy is not particularly abnormal (25).

The etiology of AS can be divided into two broad groups (Figure 1). The first group, nondeletion AS, mainly affects the function of *UBE3A*. Nondeletion AS, comprising 25% to 30% of all AS cases, includes *UBE3A* mutations, imprinting defects, and paternal uniparental disomy (7,26). The second group, deletion AS, is defined by deletions of chromosome 15 at 15q11-q13. Deletions vary in length (7) but all encompass *UBE3A*, as well as about 11 to 15 other protein-coding genes, numerous small nucleolar RNA genes, and noncoding regions of potential functional significance. Deletion AS accounts for the majority (about 70%) of AS cases (7). Herein, we use “genotype” to refer to the two etiological groups defined above.

Individuals with deletion AS have a more severe clinical presentation than those with nondeletion AS (27–30), suggesting that deletion of genes other than *UBE3A* add to disease severity. However, differences in the pathophysiology between AS genotypes remain largely unknown. Deletions of

SEE COMMENTARY ON PAGE e45

Angelman Syndrome EEG Differs With Genotype



genotype ($n = 21$) in our study. Note that UPD features additionally biallelic expression of paternally imprinted genes (blue). Deletions of 15q11-q13 are typically between canonical break points (BPs) as indicated in the figure. Class I is a ~6-Mb deletion from BP1 to BP3 ($n = 10$) that includes four additional genes near the centromere as compared with class II (~5-Mb) deletions, which span BP2 to BP3 ($n = 24$). Together with atypical ($n = 2$) and unknown ($n = 1$) deletion classes, class I and class II deletions comprise the deletion genotype ($n = 37$) examined in our study. Both deletion classes encompass the gamma-aminobutyric acid type A receptor $\beta 3$ - $\alpha 5$ - $\gamma 3$ subunit gene cluster (i.e., *GABRB3*, *GABRA5*, and *GABRG3*), which is central to the interpretation of our results. AS, Angelman syndrome; snoRNA, small nucleolar RNA.

15q11-q13 include the *GABRB3*–*GABRA5*–*GABRG3* gene cluster, which encodes the $\beta 3$, $\alpha 5$, and $\gamma 3$ gamma-aminobutyric acid type A ($GABA_A$) receptor subunits. Given the important role of the $GABA_A$ receptor system in brain development and function, the deleted $GABA_A$ receptor subunit genes may cause important differences in AS genotypes. Indeed, several lines of evidence support this notion: 1) mice with disruptions of *Gabrb3* recapitulate AS-like phenotypes (including seizures and EEG abnormalities) (31); 2) deletion AS shows both altered cortical expression of the three $GABA_A$ receptor subunit genes (32) and reduced cortical $GABA_A$ receptor density (33) while also exhibiting grossly abnormal somatosensory evoked responses that may relate to $GABA_A$ receptor dysfunction (34); and 3) chromosome 15q11.2-q13.1 duplication (dup15q) syndrome (a neurodevelopmental disorder characterized by intellectual disability, autism, and epilepsy) is caused by duplications of 15q11.2-q13.1 (i.e., the “genetic converse” of deletion AS) and has a strong EEG phenotype characterized by excessive beta oscillations (35). These oscillations closely resemble the EEG signature of $GABA_A$ receptor-enhancing drugs (e.g., benzodiazepines) (36), thereby implicating the *GABRB3*–*GABRA5*–*GABRG3* gene cluster in the dup15q syndrome pathology and phenotype.

Given that the $GABA$ system is critically involved in shaping neuronal dynamics, including oscillatory processes (37–39), EEG should provide a suitable tool to capture $GABA_A$ receptor-related abnormalities in deletion AS.

AS is characterized by a strongly abnormal EEG (18,22–24). Vendrame *et al.* (23) described EEG abnormalities in a large sample of 115 individuals with AS (here, we analyze a subset of these individuals; see Methods and Materials) and found intermittent rhythmic delta oscillations (83.5%), interictal epileptiform discharges (74.2%), intermittent rhythmic theta oscillations (43.5%), and posterior rhythm slowing (43.5%). More recently, Sidorov *et al.* (18) used quantitative analyses of AS EEGs and demonstrated excess power in the delta frequency band. However, these AS EEG abnormalities have been reported for both deletion and nondeletion AS genotypes. Comparing EEG differences between deletion and nondeletion AS may provide valuable insights into the

Figure 1. Schematic of 15q11-q13. The maternally expressed (i.e., paternally imprinted in neurons) gene *UBE3A* is shown in red, paternally expressed (i.e., maternally imprinted in neurons) genes are shown in blue. Genes shown in black are non-imprinted (i.e., biallelically expressed); n indicates the number of participants for different genotypes. *UBE3A* mutations ($n = 10$), paternal uniparental disomy (UPD) ($n = 4$), imprinting defects ($n = 5$), could either be deletion within the imprinting center or an abnormal epigenetic imprint), and abnormal DNA methylations that are not deletions (could be either UPD or imprinting defects, $n = 2$) primarily affect *UBE3A*. These etiologies comprise the nondeletion

respective contributions of *UBE3A* and non-*UBE3A* neuronal pathophysiology but has not yet been quantitatively investigated.

Here we compared EEG power spectra between deletion and nondeletion AS. Considering the foregoing evidence, we tested two specific hypotheses concerning deletion AS compared with nondeletion AS: 1) stronger power in the delta frequency band and 2) weaker power in the beta frequency band, i.e., the opposite of the EEG phenotype observed in both dup15q syndrome (35) and healthy individuals challenged with positive $GABA_A$ receptor modulators (36). We then explored a broad range of EEG frequencies in a data-driven manner.

METHODS AND MATERIALS

See the [Supplemental Methods and Materials](#) for an extended description of the methods.

Data Collection

EEG recordings were obtained from patients with AS through the AS Natural History Study [NCT00296764; a subset of the data has been analyzed previously (18,23)] (see [Supplemental Methods](#) for more information). EEG recordings from a control group of children with typical development (TD) who had tested negative for neurological or developmental concerns were obtained through Boston Children’s Hospital. Consent was obtained according to the Declaration of Helsinki and was approved by the institutional review boards of the participating sites. EEG data were acquired in a clinical setting using an international 10–20 system. Data presented here are from children and adolescents, i.e., participants with ages between 12 and 216 months (1–18 years) recorded in the awake state. The awake state was not further controlled with respect to eye condition (e.g., eyes open or eyes closed), as the ages and developmental abilities of many participants precluded complying with such instructions. A total of 144 datasets entered preprocessing.

Preprocessing

EEG data were bandpass filtered 0.5 to 45 Hz (finite impulse response filter), then portions of the data containing gross

artifacts, as well as bad channels, were identified by visual inspection and excluded from analysis. Ten datasets were excluded for overall insufficient data quality. Independent component analysis was applied to remove remaining artifacts [FastICA algorithm (40,41)]. Finally, rejected channels were interpolated and data were re-referenced to average. The final dataset analyzed included 127 recordings from 106 participants. The average individual dataset length was 15.9 ± 8.36 minutes. See [Supplemental Table S1](#) for a summary of retained data by genotype and testing site.

Frequency Transform

Power spectral estimates were derived for logarithmically scaled frequencies ranging from 1 to 32 Hz ($f/\sigma_f = 8.7$) using Morlet wavelets (42). Absolute power values were then scaled and log-transformed to have units $10 \cdot \log_{10}(\mu V^2 / \log_2(\text{Hz}))$. Consequently, differences between signals are in decibels. For analyses of relative power, data were expressed in units of $1/\log_2(\text{Hz})$.

Peak Frequencies

Peak frequencies were determined within predefined frequency ranges (delta: 1.5–4 Hz; theta: 4–8 Hz). Additionally, we reported the “center of mass,” derived as the weighted average value of the frequency within the two frequency ranges.

Statistical Analyses

For statistical analysis, we used the following linear mixed model (LMM) (43) and variants with less fixed factors:

$$P \sim 1 + \text{GENOTYPE} + \text{AGE} + \text{GENOTYPE} : \text{AGE} \\ + (1|\text{PARTICIPANT})$$

where P is log-transformed power in a given frequency band, AGE is the \log_2 -transformed and mean-centered age, and GENOTYPE contains categorical variables [AS, TD], [deletion, nondeletion], or [deletion class I, deletion class II].

To derive 95% confidence intervals for illustration and to test specific hypotheses, we used t tests within LMMs. To test for relevance of factors (e.g., GENOTYPE or AGE), we used log-likelihood ratio tests between nested models. To correct for multiple comparisons when performing analyses across all frequencies, we additionally applied a random permutation approach (44). Finally, to evaluate stability of the delta-band EEG power, we used the intraclass correlation coefficient derived from the first two visits of participants with more than one visit (45).

RESULTS

We obtained clinical EEG data in the awake state from children and adolescents (1–18 years of age) with AS and TD control participants. After preprocessing and quality control, we retained 49 datasets from 37 individuals (10 female participants) with deletion AS, 30 datasets from 21 individuals (6 female participants) with nondeletion AS, and single-visit datasets from 48 TD control participants (22 female participants) (Figure 1). There is an overrepresentation of male participants in the AS sample that is close to significance compared with the TD control participants ($p = .054$, χ^2 test). This is likely due to chance, given that AS is an autosomal disorder with no known difference in prevalence between

sexes. Importantly, the sex ratio did not differ between AS genotypes ($p = .90$, χ^2 test). In line with previous reports, participants with AS presented with global developmental delay, lack of speech, and epilepsy (see [Supplemental Figure S1](#)). Mean age (averaged across multiple visits; deletion AS: 4.6 ± 3.0 years, nondeletion AS, 7.3 ± 3.3 years, TD control participants: 8.8 ± 5.0 years) differed significantly between AS genotypes ($p = 1.66 \times 10^{-4}$) and between AS and TD cohorts ($p = 2.50 \times 10^{-3}$). Age was accounted for in the subsequent analyses.

Spectral Power Differs Between AS and TD Control Participants

We first investigated differences in EEG spectral power between AS (combined deletion and nondeletion genotypes) and TD control participants. For each visit of each participant, we derived spectral power estimates (1–32 Hz), averaged across electrodes, and fitted LMMs for each frequency separately (see Methods and Materials). To test for differences between participants with AS and TD control participants, we compared the model to a nested model lacking diagnosis (AS, TD) information. Importantly, the models accounted for age and repeated visits of the same individuals. We found that spectral power differed between AS and TD control participants for all frequencies (i.e., AS vs. TD labels significantly contributed to the model fit; $p < .05$, random permutation test, corrected for all frequencies).

To understand the directionality of the difference in spectral power, we set the age in the model to the mean \log_2 age (5.4 years) and investigated group differences. We found higher power for AS compared with TD control participants across all frequencies (Figure 2A; [Supplemental Figure S2A](#)). The largest difference manifested in a prominent peak in the delta frequency range (peak frequency = 2.8 Hz, Cohen's $d = 1.22$, power difference AS vs. TD: 11.1 dB or 1182%). Excess power in the delta frequency was a global phenomenon visible at all electrodes, demonstrating the largest effect size at temporal electrodes (Figure 2B, C; [Supplemental Figure S2B](#)). A total of 16 AS participants had at least two separate EEG assessments (12.9 ± 3.11 months apart), allowing us to investigate stability. The delta-band EEG power had moderate stability (intraclass correlation coefficient: 0.68) (see [Supplemental Figure S2C](#)). While excess power was most prominent in the delta frequency range, power was broadly elevated. Testing total power (i.e., integrating power over all frequencies) yielded a similar effect size between the AS and TD groups (see [Supplemental Table S2](#) for full details; [Supplemental Figure S2D](#)).

It is well established in typical development that absolute EEG power at all frequencies decreases with age, while the relative power at higher frequencies (>8 Hz) increases (46,47). We next investigated the developmental trajectory of AS delta power in terms of both power and peak frequency, i.e., the two key quantities characterizing oscillatory processes. Power at the AS group-level delta peak frequency exhibited a significant decline with age in both groups (Figure 2D) (TD group: -3.17 dB/oct, $p = 3.85 \times 10^{-8}$; AS group: -4.20 dB/oct, $p = 4.21 \times 10^{-12}$) (LMM parameters in [Supplemental Table S3](#) for full details). Slopes did not differ significantly between AS and TD control participants (difference: -1.03 dB/oct, $p = .202$). Clear delta peaks could be identified in 70 EEG recordings from 54 of

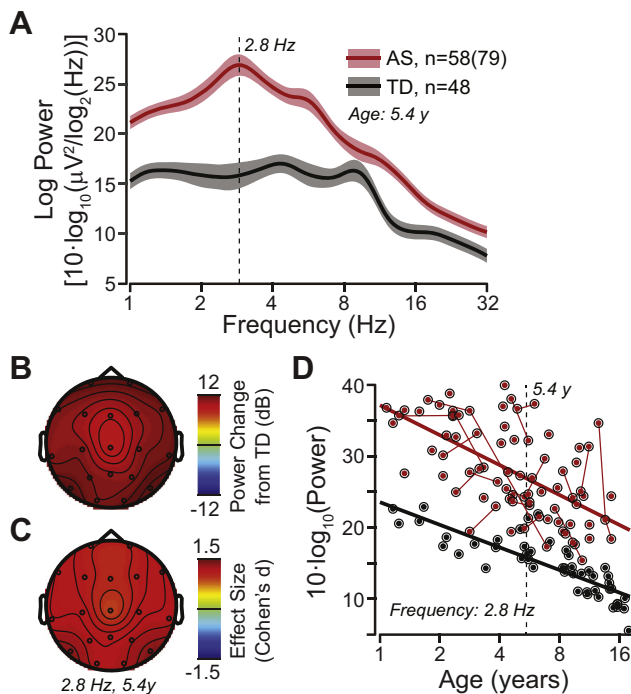


Figure 2. Spectral power differences between Angelman syndrome (AS) and typically developing (TD) control participants. **(A)** Grand average power spectral density derived from the linear mixed model, with age set to the mean \log_2 age of 5.4 years (average across all visits and electrodes). AS: red, TD control participants: black. The colored bands show 95% confidence intervals. **(B, C)** Scalp topography of power change in decibels and effect size (Cohen's d) between AS and TD control participants derived from the linear mixed model for 2.8 Hz (i.e., AS delta peak frequency) and the mean \log_2 age of 5.4 years. **(D)** Developmental trajectory of channel-averaged delta power (2.8 Hz) derived from the linear mixed model. Longitudinal visits are connected by solid lines.

58 participants with AS (Supplemental Figure S5A). The delta peak frequency was not associated with age (LMM, log-likelihood ratio test of model with and without age, $p = .492$). Center of mass, an alternative metric for quantifying the dominant frequency, also showed no relationship with age (frequency range: 1.5–4 Hz, $p = .832$). Thus, the excess EEG delta power in AS decreases during development at a similar rate as TD control participants and consequently remains at a higher baseline throughout development.

Excess power in the delta frequency range is in line with previous reports of excess relative delta power in AS compared with TD control participants (18). Our results show that power is increased across all frequencies analyzed (1–32 Hz) and exhibits the strongest difference in the delta frequency range. Consequently, the effect size is larger for absolute power compared with relative power (absolute power: Cohen's $d = 1.22$, relative power: Cohen's $d = 0.67$; at delta peak frequency, 2.8 Hz) (see Supplemental Figure S3 for the analysis of relative power).

Spectral Power Differs Between AS Genotypes

To investigate phenotypic differences in EEG spectral power between AS subtypes, we split the AS group into deletion AS ($n = 34$, participants with class I or class II deletion) and non-deletion AS ($n = 21$) subgroups. First, we tested the two

specific hypotheses as outlined in the introduction. A comparison of delta power between AS deletion genotypes (hypothesis 1) at the AS group level peak frequency (2.8 Hz) revealed 2.97-dB higher power compared with the AS non-deletion genotype at mean \log_2 age of 4.7 years (corresponding to 198.3% power relative to nondeletion AS) (Figure 3A) ($p = .0498$, two-tailed t test) (LMM parameters in Supplemental Table S4 for full details). The power differences decline with age and were greatest over temporal scalp regions (Figure 3B, C). A comparison of beta power in AS deletion genotypes at the dup15q syndrome peak frequency [hypothesis 2; 23 Hz (35)] revealed -1.69 dB lower power compared with nondeletion AS at mean \log_2 age of 4.7 years (corresponding to 67.7% relative to nondeletion AS) (Figure 4A) ($p = .0168$, two-tailed t test) (LMM parameter in Supplemental Table S5 for full details). Power differences at 23 Hz were greatest over central scalp regions (Figure 4B, C). Thus, the AS deletion genotype exhibits stronger delta power but weaker beta power than the nondeletion AS genotype. The latter observation in the AS deletion genotype resembles an inversion of the dup15q syndrome EEG phenotype (35).

Next, we switched to an exploratory analysis and tested for AS genotype differences in an unbiased and data-driven manner across the full frequency range. This analysis revealed highly significant excess theta-band power of 5.20 dB centered at 5.3 Hz for deletion AS compared with nondeletion AS (corresponding to 331% of the nondeletion AS value) (Figure 5A, B; Supplemental Figure S4A–C) ($p < .01$) (LMM-based random permutation test corrected for multiple comparisons across frequencies and accounting for age, LMM parameter for 5.3 Hz in Supplemental Table S6). A local maximum existed in theta-band only for deletion AS but not for nondeletion AS. Power differences in 5.3 Hz power were greatest over centroparietal regions (Figure 5E–G). In sum, these results suggest that the EEG phenotype of deletion AS is characterized by an oscillation in the theta frequency range that is absent in nondeletion AS.

We then investigated the developmental trajectory of the theta-band deletion AS phenotype in terms of both power and

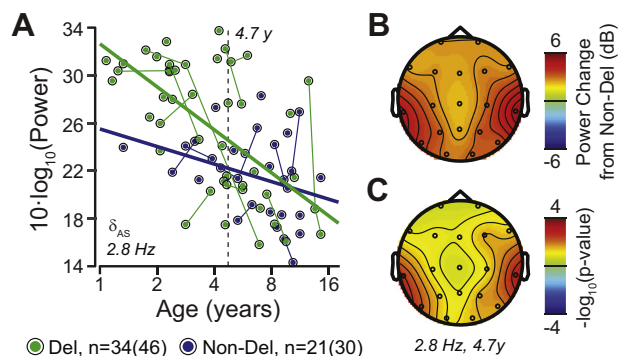


Figure 3. Spectral power in the delta frequency band differs between Angelman syndrome (AS) genotypes. **(A)** Developmental trajectory of electrode-averaged delta power (2.8 Hz) derived from the linear mixed model (average across all electrodes). Deletion AS (Del) is shown in green, non-deletion AS (Non-Del) is shown in blue. Longitudinal visits are connected by solid lines. **(B, C)** Scalp topography of power change in decibels and p values for t tests between deletion AS and nondeletion AS derived from the linear mixed model for 2.8 Hz and the mean \log_2 age of 4.7 years.

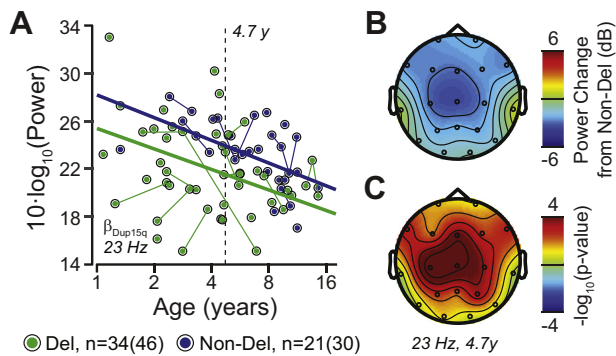


Figure 4. Spectral power in the beta frequency band differs between Angelman syndrome (AS) genotypes. **(A)** Developmental trajectory of electrode-averaged beta power [23 Hz according to hypothesis 2; i.e., peak frequency derived from chromosome 15q11.2-q13.1 duplication syndrome electroencephalography phenotype (35)] derived from the linear mixed model (average across all electrodes). Deletion AS (Del) is shown in green, nondeletion AS (Non-Del) is shown in blue. Longitudinal visits are connected by solid lines. **(B, C)** Scalp topography of power change in decibels and p values for t tests between deletion AS and nondeletion AS derived from the linear mixed model for 23 Hz and the mean \log_2 age of 4.7 years.

peak frequency (Figure 5C). We found a significant decrease in theta power (5.3 Hz) with age for deletion AS (slope: -2.26 dB/oct, $p = 3.45 \times 10^{-4}$) but not for nondeletion AS (slope: -1.27 dB/oct, $p = .185$). This suggests a developmental decline of the deletion AS theta-band oscillation. However, slopes did not significantly differ between AS subgroups (difference in slope: -0.99 dB/oct, $p = .381$) (see Supplemental Figure S4E for topography).

Clear theta peaks could be identified in 37 EEG recordings from 28 of 34 participants with class I or class II deletion AS (participants with atypical deletions were excluded) (Supplemental Figure S5B). For participants with theta peaks, we found a significant increase of 0.31 dB/oct in peak frequency with age (LMM, log-likelihood ratio test of model with and without age, $p = .011$) (Figure 5D). This finding was confirmed

using an alternative approach that quantifies the dominant frequency, i.e., center of mass, which can be derived for all deletion AS participants ($p = 8.70 \times 10^{-5}$, slope: 0.15 Hz/oct) (see Supplemental Figure S4D). Thus, the deletion AS theta oscillations increase in frequency over the course of development.

The deletion group can be further broken down into subgroups with different deletion size [class I: ~ 6 Mb; class II: ~ 5 Mb; we excluded rare atypical deletions from analysis (7,48)]. However, we did not find an improved model fit when adding deletion subclass information, even when ignoring the correction for multiple testing across frequencies ($p > .05$, log-likelihood ratio tests). Notably, both deletion subgroups encompass the *GABRB3-GABRA5-GABRG3* gene cluster. This suggests that the genes responsible for driving the differences between deletion AS and nondeletion AS reside in the region shared by deletion classes I and II.

To examine potential confounders introduced by medication, we categorized all medications taken by participants that either 1) act principally on the central nervous system or 2) have incidental central nervous system side effects. Medications were classified by a physician, and further subcategories were established for central nervous system medications: antiepileptics, antipsychotics, alpha agonists, and stimulants. For each category and subcategory, we calculated the proportion of participants in each AS genotype taking a medication during at least one EEG recording used in our analysis (Table 1; Supplemental Figure S6). Chi-square tests did not reveal differences between AS genotypes, suggesting that differences in EEG reflect differences in pathophysiology rather than medication.

DISCUSSION

Our findings demonstrate a robust electrophysiological phenotype in children with AS and reveal several frequency-specific differences between deletion and nondeletion AS genotypes. In the following, we summarize phenotypic differences, link them to GABAergic signaling, and discuss practical implications for the use of EEG as a biomarker.

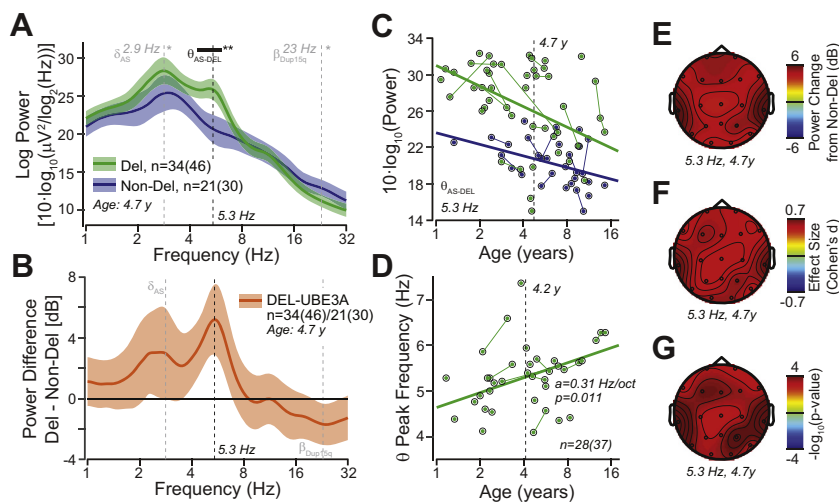


Figure 5. Spectral power differs between Angelman syndrome (AS) genotypes. **(A)** Grand average power spectral density derived from the linear mixed model with age set to the mean \log_2 age of 4.7 years (average across all visits and electrodes). Deletion AS (Del) is shown in green, nondeletion AS (Non-Del) is shown in blue. The colored bands show 95% confidence intervals. The black bar indicates frequency ranges with significant group differences (corrected for multiple testing across frequencies). The gray lines indicate the specific hypotheses tested in the delta and beta bands (see Figures 3 and 4). **(B)** Difference in spectral power between deletion AS and nondeletion AS. The colored bands show 95% confidence intervals. **(C)** Developmental trajectory of theta power (5.3 Hz) derived from the linear mixed model (average across all electrodes). Longitudinal visits are connected by solid lines. **(D)** Correlation between theta peak frequency and age. Longitudinal visits are connected by solid lines. **(E-G)** Scalp topography of power change in decibels, effect size (Cohen's d), and p values for t tests between deletion AS and nondeletion AS derived from the linear mixed model for 5.3 Hz and the mean \log_2 age of 4.7 years.

decibels, effect size (Cohen's d), and p values for t tests between deletion AS and nondeletion AS derived from the linear mixed model for 5.3 Hz and the mean \log_2 age of 4.7 years.

Table 1. Medication Overview

Drug Type	Nondeletion Participants	Nondeletion Recordings	Deletion Participants	Deletion Recordings	χ^2 (df)	p Value
CNS	16 (76.2)	23	28 (76)	39	1.939 (1)	.965
AED	11 (52.4)	17	26 (70)	36	1.856 (1)	.173
AP	2 (9.5)	2	1 (3)	2	1.271 (1)	.260
CSE	5 (23.8)	7	7 (19)	11	0.195 (1)	.659
AA	3 (14.3)	4	3 (8)	5	0.551 (1)	.458
STM	1 (4.8)	1	0 (0)	0	1.793 (1)	.181

Values are n (%). This table summarizes the proportion of nondeletion Angelman syndrome and deletion Angelman syndrome participants on each of six different medication types. Proportions are calculated from the number of unique participants in a group taking the medication at one or more electroencephalography recording sessions used in the analysis. The number of affected participants and electroencephalography recordings are reported in separate columns.

AA, alpha agonist; AED, antiepileptic drug; AP, antipsychotic; CNS, central nervous system; CSE, central nervous system side effects; STM, stimulant.

Excess Delta-Band Oscillations Are a Robust UBE3A-Related AS Phenotype

We found excess delta oscillations to be the most prominent AS EEG phenotype. This result agrees with clinical observations of qualitatively abnormal EEG activity in AS (22,49,50) and a recent publication by Sidorov *et al.* (18) that demonstrated a robust increase in relative power in the same frequency range. Our results extend previous work in several directions. First, we showed that EEG power is elevated across a broad range of frequencies (i.e., all frequencies analyzed, 1–32 Hz) and, consequently, absolute delta power better separates AS and TD control participants as compared with relative delta power. The origin of this frequency-unspecific increase of EEG signal power is unknown, and it is unclear if it relates to neurophysiological or, alternatively, anatomical abnormalities (e.g., altered tissue conductivities; though somatic and head growth are relatively normal in AS) (see Supplemental Figure S1). Second, we characterized the developmental trajectory across a broad age range (1–18 years) and showed that delta power increase (relative to TD control participants) is stable across development. Third, we found that the delta-band AS phenotype is more pronounced for deletion as compared with nondeletion AS at young ages, though future studies with better age-matched data at younger ages are needed to elaborate on this finding. Last, we showed the delta-band power increase in AS is widespread but strongest at temporal electrodes. The pathophysiological mechanisms underlying the delta-band EEG phenotype are unknown; nonetheless, our results provide some insights. The observation that the delta EEG phenotype is present in both deletion and nondeletion AS suggests that it is driven by downstream effects of UBE3A disruption. For instance, tonic GABAergic inhibition impaired through disruption of UBE3A-dependent GABA transporter 1 degradation (GAT1) (51) might underlie the delta EEG phenotype. However, it is well established both preclinically (12–17) and clinically (20,21) that the lack of UBE3A leads to cellular abnormalities and impaired synaptic function, which in turn may manifest in the observed abnormal delta activity.

Theta- and Beta-Band Oscillations Index Non-UBE3A Pathophysiology in Deletion AS Implicating the GABRB3-GABRA5-GABRG3 Gene Cluster

First, we confirmed the hypothesis, put forward in the introduction, that beta-band power is decreased in deletion AS compared with nondeletion AS. This builds on recent work in

dup15q syndrome (35,52) suggesting that EEG beta-band activity reflects a gene-dose effect of the three GABA_A receptor subunit genes (*GABRA5*, *GABRB3*, and *GABRG3*) manifesting in altered GABA_A receptor density and, consequently, in altered network dynamics. These changes in the beta frequency band likely reflect abnormalities in recurrent excitatory-inhibitory feedback loops in cortical tissue (53,54) and are well in line with pharmacological effects of GABA_A receptor modulators (36). Notably, the spatial topographies of the beta-band modulation in dup15q syndrome and AS are very different (Figure 4B, C) [cf. Figure 2 in Frohlich *et al.* (35)]. This may be expected if certain brain areas start from a state where beta oscillations can be upregulated, but not downregulated, while other brain areas start from a state where beta oscillations can be downregulated, but not further upregulated. Although the cortical networks underlying our finding remain unknown, the observation of lower beta power in the deletion AS genotype nonetheless adds to the rationale for targeting GABA_A receptors in the group of neurodevelopmental disorders affecting the *GABRB3-GABRA5-GABRG3* gene cluster (e.g., AS, Prader-Willi syndrome, and dup15q syndrome).

The most prominent difference between AS genotypes, however, was not anticipated by our hypotheses: oscillatory activity in the theta frequency range, which is present only for the deletion AS genotype. Rhythmic theta in AS has been qualitatively described in previous publications (23,24,55,56), but to the best of our knowledge, our work is the first to quantify excess theta oscillations and to link them to the deletion AS genotype. Given that GABA_A receptors are critically involved in shaping neuronal dynamics reflected in EEG oscillations (37–39), deletion of the *GABRB3-GABRA5-GABRG3* gene cluster is the most likely cause of the AS genotype differences observed in our study. However, we cannot rule out contributions from genes common to both deletion classes beyond the *GABRB3-GABRA5-GABRG3* gene cluster, though EEG effects related to these other genes are unknown. Other important 15q11-q13 genes that are not shared by the two major deletion classes (class I and class II), e.g., *CYFIP1*, can be effectively ruled out as explanations for the EEG effect within the limits of the statistical power of our study.

GABA_A Receptor Hypothesis Provides Testable Predictions

As outlined above, our results suggest that deletion of the *GABRB3-GABRA5-GABRG3* gene cluster underlies the

electrophysiological differences between AS deletion and non-deletion genotypes. This GABA_A receptor hypothesis provides specific, falsifiable predictions. For instance, our work makes testable predictions concerning EEG abnormalities that should be observable in Prader-Willi syndrome, a neurogenetic disorder caused by either a paternal 15q11-q13 deletion or maternal uniparental disomy of chromosome 15 (57), and suggests pre-clinical experiments in knockout animals that investigate the effect of *Ube3a* and GABA-subunit gene loss in isolation and in combination (see [Supplemental Discussion](#) for more details).

EEG as a Biomarker of AS

Understanding the AS EEG phenotype also has important practical implications for the development of treatments. For successful clinical development of a potential treatment, biomarkers that quantify the disease pathophysiology and provide an objective indicator of treatment response are of critical importance (58). EEG has been suggested as a promising quantitative, robust, and translatable biomarker for AS (18). Highly targeted AS treatments (e.g., antisense oligonucleotides) acting specifically on *UBE3A* expression (59–61) require biomarkers to demonstrate target engagement and treatment effects. Our findings provide evidence that the delta-band EEG abnormality indexes *UBE3A*-related pathophysiology, while the theta-band and beta-band EEG abnormalities index contributions from other genes, most likely the *GABRB3-GABRA5-GABRG3* gene cluster. Thus, if re-expression of *UBE3A* is the main target of the treatment, EEG delta-band power should be explored as a biomarker, whereas if the GABA_A receptors are the target, theta and beta power should be considered as biomarkers.

Conclusions

Our results suggest that hemizyosity of genes encoding GABA_A receptor subunits modulates the *UBE3A*-related electrophysiological phenotype and causes widespread changes in cortical dynamics, manifesting as spectrally specific abnormalities in oscillatory neuronal activity. These electrophysiological abnormalities may underlie the more severe behavioral phenotype of deletion AS. Our work has direct implications for the use of EEG as a biomarker in the development of treatments for AS.

ACKNOWLEDGMENTS AND DISCLOSURES

This work was supported by National Institutes of Health (NIH) Grant Nos. U54RR019478 (LMB, W-HT: principal investigator, Arthur Beaudet) and U54HD061222 (LMB, W-HT: principal investigator, Alan Percy); NIH National Institute of Mental Health Grant No. R01MH100186 (to AR); NIH National Institute of Neurological Disorders and Stroke Grant Nos. R01NS088583 (to AR) and R01NS100766 (to AR); the Translational Research Program at Boston Children's Hospital; and NIH National Institute of Child Health and Human Development Grant No. R01HD093771 (to BDP).

We thank the children and families who participated in this study for their generosity. Our work would not be possible without their involvement. We are also indebted to Nima Chenari for contributing the artwork in [Figure 1](#).

MTM, PG, MCH, M-CH, MK, OK, and JFH are full-time employees of F. Hoffmann-La Roche Ltd. JF is a former employee of F. Hoffmann-La Roche Ltd. (until July 2017); SSJ, BDP, and AR serve as consultants for and have received funding from F. Hoffmann-La Roche Ltd. All other authors report no biomedical financial interests or potential conflicts of interest.

ClinicalTrials.gov: Characterization of Angelman Syndrome; <https://clinicaltrials.gov/ct2/show/NCT00296764>; NCT00296764.

ARTICLE INFORMATION

From Neuroscience Ophthalmology and Rare Diseases (JF, MTM, PG, MCH, M-CH, MK, OK, JFH), Roche Innovation Center, Roche Pharma Research and Early Development, Basel, Switzerland; Center for Autism Research and Treatment (JF, SSJ), Semel Institute for Neuroscience, University of California, Los Angeles, Los Angeles; and Department of Pediatrics (LMB), University of California, San Diego; and Division of Genetics/Dysmorphology (LMB), Rady Children's Hospital San Diego, San Diego; Department of Neurology (HP, AR) and Division of Genetics and Genomics (W-HT), Boston Children's Hospital, Harvard Medical School, Boston, Massachusetts; and the Neuroscience Center (BDP, MSS), Carolina Institute for Developmental Disabilities; and Department of Cell Biology and Physiology (BDP, MSS), University of North Carolina at Chapel Hill, Chapel Hill, North Carolina.

Address correspondence to Joel Frohlich, Ph.D., University of California, Los Angeles, Franz Hall, 502 Portola Plaza, Los Angeles, CA 90095; E-mail: joelfrohlich@gmail.com; or Joerg F. Hipp, Ph.D., Roche Pharma Research and Early Development, Neuroscience, Ophthalmology and Rare Diseases, Roche Innovation Center Basel, Grenzacherstrasse 124, CH-4070 Basel, Switzerland; E-mail: joerg.hipp@roche.com.

Received Sep 4, 2018; revised Dec 11, 2018; accepted Jan 4, 2019.

Supplementary material cited in this article is available online at <https://doi.org/10.1016/j.biopsych.2019.01.008>.

REFERENCES

- Mertz LGB, Christensen R, Vogel I, Hertz JM, Nielsen KB, Grønskov K, Østergaard JR (2013): Angelman syndrome in Denmark. Birth incidence, genetic findings, and age at diagnosis. *Am J Med Genet A* 161:2197–2203.
- Petersen MB, Brøndum-Nielsen K, Hansen LK, Wulff K (1995): Clinical, cytogenetic, and molecular diagnosis of Angelman syndrome: Estimated prevalence rate in a Danish county. *Am J Med Genet* 60:261–262.
- Williams CA (1995): Angelman syndrome: Consensus for diagnostic criteria. *Am J Med Genet* 56:237–238.
- Trillingsgaard A, Østergaard JR (2004): Autism in Angelman syndrome: An exploration of comorbidity. *Autism* 8:163–174.
- Thibert RL, Larson AM, Hsieh DT, Raby AR, Thiele EA (2013): Neurologic manifestations of Angelman syndrome. *Pediatr Neurol* 48:271–279.
- Bird LM (2014): Angelman syndrome: Review of clinical and molecular aspects. *Appl Clin Genet* 7:93.
- Buiting K, Williams C, Horsthemke B (2016): Angelman syndrome—insights into a rare neurogenetic disorder. *Nat Rev Neurol* 12:584–593.
- Chamberlain SJ, Lalonde M (2010): Angelman syndrome, a genomic imprinting disorder of the brain. *J Neurosci* 30:9958–9963.
- Kishino T, Lalonde M, Wagstaff J (1997): *UBE3A/E6-AP* mutations cause Angelman syndrome. *Nat Genet* 15:70–73.
- Yamasaki K, Joh K, Ohta T, Masuzaki H, Ishimaru T, Mukai T, et al. (2003): Neurons but not glial cells show reciprocal imprinting of sense and antisense transcripts of *Ube3a*. *Hum Mol Genet* 12:837–847.
- Albrecht U, Sutcliffe JS, Cattanach BM, Beechey CV, Armstrong D, Eichele G, Beaudet AL (1997): Imprinted expression of the murine Angelman syndrome gene, *Ube3a*, in hippocampal and Purkinje neurons. *Nat Genet* 17:75–78.
- Dindot SV, Antalffy BA, Bhattacharjee MB, Beaudet AL (2008): The Angelman syndrome ubiquitin ligase localizes to the synapse and nucleus, and maternal deficiency results in abnormal dendritic spine morphology. *Hum Mol Genet* 17:111–118.
- Kim H, Kunz PA, Mooney R, Philpot BD, Smith SL (2016): Maternal loss of *Ube3a* impairs experience-driven dendritic spine maintenance in the developing visual cortex. *J Neurosci* 36:4888–4894.
- Wallace ML, Burette AC, Weinberg RJ, Philpot BD (2012): Maternal loss of *Ube3a* produces an excitatory/inhibitory imbalance through neuron type-specific synaptic defects. *Neuron* 74:793–800.
- Judson MC, Wallace ML, Sidorov MS, Burette AC, Gu B, van Woerden GM, et al. (2016): GABAergic neuron-specific loss of *Ube3a* causes Angelman syndrome-like EEG abnormalities and enhances seizure susceptibility. *Neuron* 90:56–69.

Angelman Syndrome EEG Differs With Genotype

16. Yashiro K, Riday TT, Condon KH, Roberts AC, Bernardo DR, Prakash R, *et al.* (2009): Ube3a is required for experience-dependent maturation of the neocortex. *Nat Neurosci* 12:777–783.
17. Sato M, Stryker MP (2010): Genomic imprinting of experience-dependent cortical plasticity by the ubiquitin ligase gene Ube3a. *Proc Natl Acad Sci U S A* 107:5611–5616.
18. Sidorov MS, Deck GM, Dolatshahi M, Thibert RL, Bird LM, Chu CJ, Philpot BD (2017): Delta rhythmicity is a reliable EEG biomarker in Angelman syndrome: A parallel mouse and human analysis. *J Neurodev Disord* 9:17.
19. Born HA, Dao AT, Levine AT, Lee WL, Mehta NM, Mehra S, *et al.* (2017): Strain-dependence of the Angelman syndrome phenotypes in Ube3a maternal deficiency mice. *Sci Rep* 7:8451.
20. Kyriakides T, Hallam LA, Hockey A, Silberstein P, Kakulas BA (1992): Angelman's syndrome: A neuropathological study. *Acta Neuropathol* 83:675–678.
21. Jay V, Becker LE, Chan FW, Perry TL (1991): Puppet-like syndrome of Angelman: A pathologic and neurochemical study. *Neurology* 41:416–422.
22. Laan LA, Vein AA (2005): Angelman syndrome: Is there a characteristic EEG? *Brain Dev* 27:80–87.
23. Vendrame M, Loddenkemper T, Zarowski M, Gregas M, Shuhaiber H, Sarco DP, *et al.* (2012): Analysis of EEG patterns and genotypes in patients with Angelman syndrome. *Epilepsy Behav* 23:261–265.
24. Dan B, Boyd S (2003): Angelman syndrome reviewed from a neurophysiological perspective. The UBE3A-GABRB3 hypothesis. *Neuropediatrics* 34:169–176.
25. Harting I, Seitz A, Rating D, Sartor K, Zschocke J, Janssen B, *et al.* (2009): Abnormal myelination in Angelman syndrome. *Eur J Paediatr Neurol* 13:271–276.
26. Clayton-Smith J, Laan L (2003): Angelman syndrome: A review of the clinical and genetic aspects. *J Med Genet* 40:87–95.
27. Moncla A, Malzac P, Voelckel M-A, Auquier P, Girardot L, Mattei M-G, *et al.* (1999): Phenotype-genotype correlation in 20 deletion and 20 non-deletion Angelman syndrome patients. *Eur J Hum Genet* 7:131–139.
28. Lossie A, Whitney M, Amidon D, Dong H, Chen P, Theriaque D, *et al.* (2001): Distinct phenotypes distinguish the molecular classes of Angelman syndrome. *J Med Genet* 38:834–845.
29. Minassian BA, Delorey TM, Olsen RW, Philippart M, Bronstein Y, Zhang Q, *et al.* (1998): Angelman syndrome: Correlations between epilepsy phenotypes and genotypes. *Ann Neurol* 43:485–493.
30. Gentile JK, Tan W-H, Horowitz LT, Bacino CA, Skinner SA, Barbieri-Welge R, *et al.* (2010): A neurodevelopmental survey of Angelman syndrome with genotype-phenotype correlations. *J Dev Behav Pediatr* 31:592–601.
31. DeLorey T, Handforth A, Anagnostaras S, Homanics G, Minassian B, Asaturian A, *et al.* (1998): Mice lacking the $\beta 3$ subunit of the GABAA receptor have the epilepsy phenotype and many of the behavioral characteristics of Angelman syndrome. *J Neurosci* 18:8505–8514.
32. Roden WH, Peugh LD, Jansen LA (2010): Altered GABAA receptor subunit expression and pharmacology in human Angelman syndrome cortex. *Neurosci Lett* 483:167–172.
33. Holopainen IE, Metsähonkala EL, Kokkonen H, Parkkola RK, Manner TE, Nägren K, Korpi ER (2001): Decreased binding of [11C] flumazenil in Angelman syndrome patients with GABA(A) receptor beta3 subunit deletions. *Ann Neurol* 49:110–113.
34. Egawa K, Asahina N, Shiraiishi H, Kamada K, Takeuchi F, Nakane S, *et al.* (2008): Aberrant somatosensory-evoked responses imply GABAergic dysfunction in Angelman syndrome. *Neuroimage* 39:593–599.
35. Frohlich J, Senturk D, Saravanapandian V, Golshani P, Reiter LT, Sankar R, *et al.* (2016): A quantitative electrophysiological biomarker of duplication 15q11.2-q13.1 syndrome. *PLoS One* 11:e0167179.
36. Greenblatt DJ, Ehrenberg BL, Gunderman J, Locniskar A, Scavone JM, Hartz JS, Shader RI (1989): Pharmacokinetic and electroencephalographic study of intravenous diazepam, midazolam, and placebo. *Clin Pharmacol Ther* 45:356–365.
37. Wang X-J (2010): Neurophysiological and computational principles of cortical rhythms in cognition. *Physiol Rev* 90:1195–1268.
38. Steriade M, Timofeev I (2003): Neuronal plasticity in thalamocortical networks during sleep and waking oscillations. *Neuron* 37:563–576.
39. Womelsdorf T, Valiante TA, Sahin NT, Miller KJ, Tiesinga P (2014): Dynamic circuit motifs underlying rhythmic gain control, gating and integration. *Nat Neurosci* 17:1031–1039.
40. Hyvarinen A (1999): Fast ICA for noisy data using Gaussian moments. In: *Proceedings of the 1999 IEEE International Symposium on Circuits and Systems. ISCAS'99. vol. 5. Piscataway, NJ: IEEE, 57–61.*
41. Jung T-P, Makeig S, Westerfield M, Townsend J, Courchesne E, Sejnowski TJ (2000): Removal of eye activity artifacts from visual event-related potentials in normal and clinical subjects. *Clin Neurophysiol* 111:1745–1758.
42. Tallon-Baudry C, Bertrand O, Delpuech C, Pernier J (1997): Oscillatory γ -band (30–70 Hz) activity induced by a visual search task in humans. *J Neurosci* 17:722–734.
43. West BT, results search, results search (2014): *Linear Mixed Models: A Practical Guide Using Statistical Software*, 2nd ed. Boca Raton, FL: Chapman and Hall/CRC.
44. Nichols TE, Holmes AP (2002): Nonparametric permutation tests for functional neuroimaging: A primer with examples. *Hum Brain Mapp* 15:1–25.
45. McGraw KO, PS (1996): Forming inferences about some intraclass correlation coefficients. *Psychol Methods* 1:30–46.
46. Gasser T, Verleger R, Bächer P, Sroka L (1988): Development of the EEG of school-age children and adolescents. I. Analysis of band power. *Electroencephalogr Clin Neurophysiol* 69:91–99.
47. Marshall PJ, Bar-Haim Y, Fox NA (2002): Development of the EEG from 5 months to 4 years of age. *Clin Neurophysiol* 113:1199–1208.
48. Finucane BM, Lusk L, Arkilo D, Chamberlain S, Devinsky O, Dindot S, *et al.* (2016): 15q Duplication Syndrome and Related Disorders. Seattle, WA: Gene Reviews.
49. Williams CA (2005): Neurological aspects of the Angelman syndrome. *Brain Dev* 27:88–94.
50. Boyd S, Harden A, Patton M (1988): The EEG in early diagnosis of the Angelman (happy puppet) syndrome. *Eur J Pediatr* 147:508–513.
51. Egawa K, Kitagawa K, Inoue K, Takayama M, Takayama C, Saitoh S, *et al.* (2012): Decreased tonic inhibition in cerebellar granule cells causes motor dysfunction in a mouse model of Angelman syndrome. *Sci Transl Med* 4:163ra157.
52. Urraca N, Cleary J, Brewer V, Pivnick EK, McVicar K, Thibert RL, *et al.* (2013): The interstitial duplication 15q11.2-q13 syndrome includes autism, mild facial anomalies and a characteristic EEG signature. *Autism Res* 6:268–279.
53. Jensen O, Goel P, Kopell N, Pohja M, Hari R, Ermentrout B (2005): On the human sensorimotor-cortex beta rhythm: Sources and modeling. *Neuroimage* 26:347–355.
54. Whittington MA, Traub RD, Kopell N, Ermentrout B, Buhl EH (2000): Inhibition-based rhythms: Experimental and mathematical observations on network dynamics. *Int J Psychophysiol* 38:315–336.
55. Sugimoto T, Yasuhara A, Ohta T, Nishida N, Saitoh S, Hamabe J, Niikawa N (1992): Angelman syndrome in three siblings: Characteristic epileptic seizures and EEG abnormalities. *Epilepsia* 33:1078–1082.
56. Valente KD, Andrade JQ, Grossmann RM, Kok F, Fridman C, Koiffmann CP, Marques-Dias MJ (2003): Angelman syndrome: Difficulties in EEG pattern recognition and possible misinterpretations. *Epilepsia* 44:1051–1063.
57. Cassidy SB, Driscoll DJ (2009): Prader-Willi syndrome. *Eur J Hum Genet* 17:3–13.
58. Jeste SS, Frohlich J, Loo SK (2015): Electrophysiological biomarkers of diagnosis and outcome in neurodevelopmental disorders. *Curr Opin Neurol* 28:110–116.
59. Matsuura T, Sutcliffe JS, Fang P, Galjaard R-J, Jiang Y, Benton CS, *et al.* (1997): De novo truncating mutations in E6-AP ubiquitin-protein ligase gene (UBE3A) in Angelman syndrome. *Nat Genet* 15:74–77.
60. Meng L, Ward AJ, Chun S, Bennett CF, Beaudet AL, Rigo F (2015): Towards a therapy for Angelman syndrome by targeting a long non-coding RNA. *Nature* 518:409–412.
61. Bishop KM (2017): Progress and promise of antisense oligonucleotide therapeutics for central nervous system diseases. *Neuropharmacology* 120:56–62.